BJP British Journal of Pharmacology

DOI:10.1111/bph.12011
www.brjpharmacol.org

RESEARCH PAPER

The inhibitor of volume-regulated anion channels DCPIB activates TREK potassium channels in cultured astrocytes

L Minieri[1]*, H Pivonkova[2]*, M Caprini[1], L Harantova[2], M Anderova[2] and S Ferroni[1]

[1]*Department of Human and General Physiology, University of Bologna, Bologna, Italy, and* [2]*Department of Cellular Neurophysiology, Institute of Experimental Medicine, Academy of Sciences of the Czech Republic, Prague, Czech Republic*

Correspondence
S Ferroni, Department of Human and General Physiology, University of Bologna, Via San Donato 19/2, 40126 Bologna, Italy. E-mail: stefano.ferroni@unibo.it

*These authors contributed equally to this work.

Keywords
astroglia; neurons; two-pore-domain potassium channels; ischemia; neuroprotection

Received
11 June 2012
Revised
10 September 2012
Accepted
28 September 2012

BACKGROUND AND PURPOSE

The ethacrynic acid derivative, 4-(2-butyl-6,7-dichlor-2-cyclopentylindan-1-on-5-yl) oxobutyric acid (DCPIB) is considered to be a specific and potent inhibitor of volume-regulated anion channels (VRACs). In the CNS, DCPIB was shown to be neuroprotective through mechanisms principally associated to its action on VRACs. We hypothesized that DCPIB could also regulate the activity of other astroglial channels involved in cell volume homeostasis.

EXPERIMENTAL APPROACH

Experiments were performed in rat cortical astrocytes in primary culture and in hippocampal astrocytes *in situ*. The effect of DCPIB was evaluated by patch-clamp electrophysiology and immunocytochemical techniques. Results were verified by comparative analysis with recombinant channels expressed in COS-7 cells.

KEY RESULTS

In cultured astrocytes, DCPIB promoted the activation of a K^+ conductance mediated by two-pore-domain K^+ (K_{2P}) channels. The DCPIB effect occluded that of arachidonic acid, which activates K_{2P} channels K_{2P} 2.1 (TREK-1) and K_{2P} 10.1 (TREK-2) in cultured astrocytes. Immunocytochemical analysis suggests that cultured astrocytes express K_{2P} 2.1 and K_{2P} 10.1 proteins. Moreover, DCPIB opened recombinant K_{2P} 2.1 and K_{2P} 10.1 expressed in heterologous system. In brain slices, DCPIB did not augment the large background K^+ conductance in hippocampal astrocytes, but caused an increment in basal K^+ current of neurons.

CONCLUSION AND IMPLICATIONS

Our results indicate that the neuroprotective effect of DCPIB could be due, at least in part, to activation of TREK channels. DCPIB could be used as template to build new pharmacological tools able to increase background K^+ conductance in astroglia and neuronal cells.

Abbreviations

AA, arachidonic acid; aCSF, artificial CSF; COS-7, African green monkey kidney cell line; DCPIB, 4-(2-butyl-6,7-dichlor-2-cyclopentylindan-1-on-5-yl) oxobutyric acid; EA, ethacrynic acid; GFAP, glial fibrillary acidic protein; K_{2P} channels, open rectifier two-pore-domain K^+ channels; MCAO, middle cerebral artery occlusion; RVD, regulatory volume decrease; TRAAK, TWIK-related arachidonic acid activated K^+ channel (K_{2P} 4.1); TREK, TWIK-related K^+ channel; TREK-1, K_{2P} 2.1; TREK-2, K_{2P} 10.1; VRACs, volume-regulated anion channels

Introduction

Astrocytes, the predominant cell type in the CNS, are the cells mainly involved in brain volume homeostasis (Kimelberg, 2005). *In vivo*, they are endowed with a variety of potassium (K^+) and chloride (Cl^-) ion channels that differently contribute to cell volume regulation (Benesova *et al.*, 2012). There is clear evidence that as a result of ischaemia and oxygen glucose deprivation astrocytes swell (Benesova *et al.*, 2009) and release high amount of glutamate/aspartate (Phillis and O'Regan, 2003). Because these processes play a pivotal role in the pathogenetic mechanisms of the ischemic damage (Kimelberg *et al.*, 2004), a great effort is currently made to identify pharmacological agents able to interfere with the underlying molecular mechanisms. One of the best characterized agent that modulates these processes is the ethacrynic acid derivative, 4-(2-butyl-6,7-dichlor-2-cyclopentylindan-1-on-5-yl) oxobutyric acid (DCPIB). DCPIB was reported to block totally astroglial swelling induced in cat cerebral cortex (Bourke *et al.*, 1981). In adult rats, DCPIB caused a reduction in size of infarct volume when applied intracisternally during 2 h of middle cerebral artery occlusion (MCAO), and decreased MCAO-induced glutamate release in the penumbra (Zhang *et al.*, 2008).

DCPIB is considered the most specific and potent inhibitor of volume-regulated anion channels (VRACs) (Nilius and Droogmans, 2003). Its effect is pronounced at low concentrations with IC_{50} ~2–4 μM depending on the cell type, and it apparently does not influence any other Cl^- or K^+ channels (Decher *et al.*, 2001). In cultured astrocytes, DCPIB selectively depressed VRACs and swelling-activated excitatory amino acid release (Abdullaev *et al.*, 2006; Vazquez-Juarez *et al.*, 2009). In ischemic astrocytes *in vivo* DCPIB was reported to inhibit excitatory amino acid release likely mediated by VRACs (Feustel *et al.*, 2004). However, whether the neuroprotection offered by DCPIB is also due to its ability to modulate other ion channels involved in cell volume regulation is currently unknown.

The capacity of cells to recover their volume following a sudden increase is mediated by Cl^- and K^+ channels and ion transporters (for review see Pasantes-Morales *et al.*, 2006; Kahle *et al.*, 2009). The specific K^+ channels involved in this mechanism are still unknown. Possible candidates are the polymodal TREK channels, which belong to the two-pore-domain K^+ (K_{2P}) channel family. TREK channels including K_{2P} 2.1 (TREK-1) and K_{2P} 10.1 (TREK-2) generate outwardly rectifying K^+ currents under physiological intra- and extracellular K^+ concentrations that become linear in symmetrical K^+. TREKs are gated by cell swelling and plasma membrane stretch, moderate temperature, acidic pH, polyunsaturated fatty acids (e.g. arachidonic acid) and phosphorylation (for a review see Patel and Honore, 2001). Because they carry substantial current at very negative membrane potentials, their primary function is to maintain the cell membrane potential close to the K^+ equilibrium potential (Goldstein *et al.*, 2001). Openers of TREKs, such as volatile anaesthetics, riluzole or polyunsaturated fatty acids have been proposed as potential neuro- or cardioprotective agents (Duprat *et al.*, 2000; Lawson and McKay, 2006; Judge and Smith, 2009). The polymodal gating of TREK channels suggests that they also could be activated under pathological conditions that lead to cell swelling and/or an increase in polyunsaturated free fatty acids (Lipton, 1999).

In this study, we show that in cultured cortical astrocytes, the VRAC inhibitor DCPIB activates membrane currents displaying K_{2P} channel properties. Immunocytochemical analysis suggested the expression of K_{2P} 2.1 and K_{2P} 10.1 in cultured astroglia. The effect of DCPIB on open rectifier K^+ channels was further corroborated by the stimulatory effect of DCPIB on heterologously expressed K_{2P} 2.1 and K_{2P} 10.1. Finally, DCPIB increased the background K^+ conductance in hippocampal neurons *in situ* but not that of astrocytes, which is constitutively very large. Collectively, our findings indicate that the neuroprotective action of DCPIB could be partially mediated by its ability to open K_{2P} channels in brain cells. DCPIB could therefore represent the prototypic molecule of novel neuroprotective agents able to stimulate the neuronal and astrocytic membrane K^+ conductance. A preliminary account of this work has been presented in abstract form (Minieri *et al.*, 2011).

Methods

Preparation of primary culture of rat cortical astrocytes

The experiments were performed according to the Italian and international laws on protection of laboratory animals, with the approval of a local bioethical committee and under the supervision of a veterinary commission for animal care and comfort of the University of Bologna. Every effort was made to minimize the number of animals used and their sufferings. Primary cultures of rat cortical astrocytes were obtained as described previously (Ferroni *et al.*, 1995). Briefly, after removal of the meninges, cortical tissue of 1–2-day-old pups was triturated and placed on culture flasks. The cells were cultured in Dulbecco's modified Eagle's medium (DMEM) supplemented with 15% of heat-inactivated fetal bovine serum (FBS) and penicillin/streptomycin (100 $U \cdot mL^{-1}$ and 100 $\mu g \cdot mL^{-1}$, respectively) at 37°C in a 5% CO_2 humidified incubator and used between 3 and 5 weeks of growth (all products were obtained from Gibco-Invitrogen, Milan, Italy). Immunostaining for glial fibrillary acidic protein (GFAP) and the flat, polygonal morphological phenotype of the cultured cells indicated that more than 95% were type-1 cortical astrocytes. After reaching confluence, astrocytes were digested enzymatically by trypsin-EDTA and plated in Petri dishes at a density of $2–2.5 \times 10^4$ per dish. Electrophysiological experiments were carried out 3–5 days later.

Immunocytochemistry in primary cultured astrocytes

Cells attached to cover slips were fixed using 4% paraformaldehyde (PFA) for 15 min, washed twice and kept in 0.01 M PBS. The immunohistochemical staining was performed in a blocking solution containing 1% bovine serum albumin (BSA), 5% normal goat serum (NGS, Millipore, MA, USA) and 0.5% Triton in 0.1 M phosphate buffer (PB). Cover slips were incubated overnight at 4°C with the primary antibody diluted in the blocking solution and subsequently with the appropriate species/subclass-specific secondary antibody for

2 h at room temperature (RT). The following primary antibodies were used: mouse anti-GFAP (Cy3-conjugate; 1:800), rabbit anti-K_{2P} 2.1 (1:200, Alomone Labs, Jerusalem, Israel) and rabbit anti-K_{2P} 10.1 (1:200, Alomone Labs). The secondary antibody was goat anti-rabbit IgG conjugated with Alexa Fluor 488 (Molecular Probes, Eugene, OR, USA). To visualize the cell nuclei the cover slips were mounted using Vectashield mounting medium with DAPI (Vector Laboratories, Burlingame, CA, USA).

Transfection of recombinant TREK channels

African green monkey kidney cell line (COS-7) cells were cultured in DMEM containing 10% FBS, nonessential amino acid cocktail (0.1 mM), penicillin (50 units·mL^{-1}) and streptomycin (50 μg·mL^{-1}), grown in 100-mm Petri dishes and maintained in a humidified-atmosphere incubator at 37°C with 5% CO_2. COS-7 cells were transfected with K_{2P} 2.1/pRK5 and K_{2P} 10.1/pcDNA3.1 constructs kindly provided by Prof. Daniel Mulkey, Department of Physiology and Neurobiology, University of Connecticut (USA). The day before transfection, COS-7 cells were re-plated in 35-mm Petri dishes at a density of 2–5 × 10^4 per dish, maintained in supplemented DMEM and alternatively co-transfected with the constructs and the reporter gene enhanced yellow fluorescent protein (Clontech Laboratories, Mountain View, CA, USA) by the DEAE-dextran method (Sigma-Aldrich, Milan, Italy). Electrophysiological measurements were carried out 24–48 h post transfection (Caprini *et al.*, 2001). Fluorescent cells were visualized using an inverted microscope (Nikon Diaphot, Nikon Italy, Florence, Italy) equipped with the appropriate epifluorescence filter.

Preparation of acute brain slices

The experiments were performed in accordance with the European Communities Council Directive of November 1986 (86/609/EEC) and animal care guidelines approved by the Institute of Experimental Medicine ASCR Animal Care Committee. All efforts were made to minimize animal suffering and to reduce the number of animals used. Wistar rats (P9–15) were deeply anaesthetized with isoflurane and killed by decapitation. The brains were quickly dissected out and transversal 300-μm thick slices were cut using a vibration microtome (HM 650V, Thermo Scientific Microm, Walldorf, Germany) in cold (4°C) isolation solution containing (in mM): 110 NMDG-Cl, 3 KCl, 23 $NaHCO_3$, 1.25 Na_2HPO_4, 0.5 $CaCl_2$, 7 $MgCl_2$, 20 glucose, osmolality 290 mOsm·kg^{-1}. The slices were incubated for 30 min at 34°C in the isolation solution and then held at RT in artificial CSF (aCSF) solution containing (in mM): 122 NaCl, 3 KCl, 28 $NaHCO_3$, 1.25 Na_2HPO_4, 1.5 $CaCl_2$, 1.3 $MgCl_2$, 10 glucose, osmolality 305 mOsm·kg^{-1}. Solutions were equilibrated with 95% O_2/5% CO_2 to a final pH of 7.4. Osmolality was measured using a vapour pressure osmometer (Vapro 5520, Wescor, Logan, UT, USA).

Electrophysiological recordings in cultured astrocytes

Standard whole-cell patch-clamp recordings (Hamill *et al.*, 1981) were performed with an amplifier (EPC-7, List Electronic, Darmstadt, Germany), and the data were filtered at 2 kHz before acquisition at a sample rate of 5 kHz on a microcomputer for off-line analysis with pClamp 5 (Axon Instrument, Foster City, CA, USA) and Origin 6.0 software (MicroCal, Northampton, MA, USA). Patch pipettes were prepared from thin-walled borosilicate glass capillaries to obtain a tip resistance of 2–4 MOhms when filled with the standard internal solution composed of (in mM): 144 KCl, 2 $MgCl_2$, 5 EGTA, 10 HEPES, pH 7.2 with KOH and osmolality ~300 mOsm·kg^{-1}. The standard bath (control) solution was (in mM): 140 NaCl, 4 KCl, 2 $MgCl_2$, 2 $CaCl_2$, 10 HEPES, 5 glucose, pH 7.4 with NaOH and osmolality adjusted to ~315 mOsm·kg^{-1} with mannitol. In order to isolate the swelling-activated currents, the standard bath solution was changed for an isotonic solution containing (in mM): 118 NaCl, 4 KCl, 2 $MgCl_2$, 2 $CaCl_2$, 10 HEPES, 5 glucose, pH 7.4 with NaOH, and osmolality adjusted to ~320 mOsm·kg^{-1} by adding mannitol (about 60 mM). The hypotonic solution of ~260 mOsm·kg^{-1} was obtained by omitting mannitol from the isotonic solution. The high K^+ extracellular solution was prepared by rising the extracellular K^+ replacing Na^+ equimolarly. To isolate Cl^- currents, the extracellular solution contained (in mM): 122 CsCl, 2 $MgCl_2$, 2 $CaCl_2$, 10 2-[[1,3-dihydroxy-2-(hydroxymethyl)propan-2-yl]amino]ethanesulfonic acid (TES), 5 glucose, pH 7.4 with CsOH, and adjusted to ~320 mOsm·kg^{-1} by adding mannitol (about 60 mM), which was omitted in the hypotonic solution of about 260 mOsm·kg^{-1}. The intracellular solution was composed of (in mM): 126 CsCl, 2 $MgCl_2$, 1 EGTA, 10 TES, pH 7.2 with CsOH, and osmolality adjusted to ~290 mOsm·kg^{-1} with mannitol. Osmolality was checked with a vapour pressure osmometer (Wescor 5500, Delcon Medical Devices, Italy). Solutions were applied with a gravity-driven, local perfusion system positioned at ~100 μm of the recorded cells. 4-(2-butyl-6,7-dichloro-2-cyclo pentyl-indan-1-on-5-yl) oxobutyric acid (DCPIB; Sigma-Aldrich), arachidonic acid (AA; Sigma-Aldrich), ethacrynic acid (Sigma-Aldrich) were all dissolved in dimethylsulfoxide at concentrations 1000-fold higher than the final concentration used when diluted in the perfusing solutions. Current densities were calculated by dividing the current amplitudes by the cell capacitance obtained through the correction of the capacitive transients in the recorded cells using the analogical circuit of the patch-clamp amplifier. The zero-current potential (E_0), which reflects the resting membrane potential, was measured by switching the amplifier to the current-clamp mode. Experiments were carried out at 20–24°C.

Electrophysiological recordings in brain slices

Acute brain slices were transferred to a recording chamber mounted on the stage of an upright microscope (Axioscop, Zeiss, Gottingen, Germany) equipped with a high-resolution digital camera (AxioCam HRc, Zeiss) and electronic micromanipulators (Luigs&Neumann, Ratingen, Germany). The chamber was continuously perfused with oxygenated aCSF at a rate of 5 mL·min^{-1} at RT. Electrophysiological recordings were performed in the whole-cell configuration, using an EPC-10 patch-clamp amplifier in combination with PATCHMASTER software (HEKA Elektronik, Lambrecht/Pfalz, Germany). Patch pipettes were pulled (P-97 Flaming/Brown Micropipette Puller, Sutter Instruments, Novato, CA, USA) from borosilicate capillaries (Sutter Instruments) and filled

with a solution containing (in mM): 130 K-gluconate, 0.5 $CaCl_2$, 5 EGTA, 10 HEPES, 3 Mg-ATP and 0.3 Na-GTP; the final pH was adjusted to 7.2 with KOH. The pipette resistances were 7–10 MOhms. The membrane resistance (R_M) was calculated from the current elicited by a 10 mV test pulse hyperpolarizing the cell membrane from the holding potential of –40 to –50 mV for 50 ms, at the end of the pulse.

Immunohistochemistry in brain slices

Rats (P12) were deeply anaesthetized with isoflurane and perfused transcardially with saline followed by 4% PFA in 0.1 M PB. Brains were dissected out, post-fixed 3 h and placed stepwise in solutions with gradually increasing sucrose concentrations (10, 20, 30%) for cryoprotection. Coronal, 20-µm thick slices were prepared using a cryostat (Leica CM1850, Leica Microsystems, Wetzlar, Germany). For cell identification after the patch-clamp recording, the measured cells were filled with Alexa Fluor 488 hydrazide (0.1 mM; Molecular Probes, Eugene, OR, USA) by dialysing the cytoplasm with the patch pipette solution. Post-recording, the slices were fixed with 4% PFA in 0.1 M PB for 1 h and then kept at 4°C in PBS. The slices were incubated with 1% BSA, 5% NGS (Millipore) and 0.5% Triton in PB. This blocking solution was also used as the diluent for the antisera. The slices were incubated with the primary antibodies at 4°C overnight, and the secondary antibodies were applied for 2 h at RT. The following primary antibodies were used: mouse anti-GFAP (Cy3-conjugate; 1:800), rabbit anti-K_{2P} 2.1 (1:200, Alomone Labs) and rabbit anti-K_{2P} 10.1 (1:200, Alomone Labs). The secondary antibody was goat anti-rabbit IgG conjugated with Alexa Fluor 488 (Molecular Probes). Slices were mounted with Vectashield containing DAPI (Vector Laboratories, Burlingame, CA, USA). All chemicals were purchased from Sigma-Aldrich (St. Louis, MO, USA), unless otherwise stated.

A Zeiss 510DUO laser scanning microscope equipped with Arg/HeNe laser and 40× or 63× oil objectives was used for immunohistochemical analysis. Stacks of consecutive confocal images taken at intervals of 1 or 0.5 µm were acquired sequentially with the two lasers to avoid cross-talk between fluorescent labels. The background noise of each confocal image was reduced by averaging four image inputs. For each image stack, the gain and detector offset were adjusted to minimize saturated pixels, yet still permit the detection of weakly stained cell processes. In all cases, the pinhole was set to 1 Airy unit. Colocalization images and their maximum z projections were made using Zeiss LSM Image Browser software.

Statistical analyses

Currents elicited with families of voltage steps or by voltage ramps were analysed with Clampfit (Axon Instruments, Axon Instrument, Foster City, CA, USA) and Origin 6.0 (MicroCal, Northampton, MA, USA). The current traces were plotted with Origin software. Data are expressed as mean ± standard error of the mean (SEM) of several cells (n) for each condition. Because of possible differences in cell size, membrane currents have been normalized and are shown as current densities. The statistical analyses were performed with two-tailed Student's t-test and values of $P < 0.05$ were considered the threshold of significance.

Results

Effect of DCPIB on swelling-activated currents in rat primary cortical astrocytes

It is well known that cultured astrocytes respond to a hypotonic challenge that causes cell swelling with an increase in membrane conductance owing to activation of VRACs (Parkerson and Sontheimer, 2003; 2004). Pharmacological studies have suggested that astrocyte swelling can also elicit an increase in K^+ conductance (Pasantes-Morales *et al.*, 1994). However, electrophysiological evidence for K^+ channel activated by hypotonicity is still lacking. In order to unravel the contribution of the K^+ channels to swelling-activated currents in astroglia, primary cultured rat cortical astrocytes were exposed to hypotonic solution in the absence and presence of the putative selective blocker of VRAC currents DCPIB (10 µM) (Nilius and Droogmans, 2003). Astrocytes were clamped at the holding potential (V_h) of –40 mV, which is close to the zero-current potential under these experimental conditions ($E_0 = -34.6 \pm 2.4$ mV, $n = 6$), and a slow ramp stimulation protocol was applied from –120 mV to +80 mV (inset to Figure 1A). Upon hypotonic challenge ($\Delta = 60$ mOsm·kg^{-1}) a gradual increase in whole-cell currents within the entire range of membrane potentials and a positive shift in E_0 to -19.2 ± 2.6 mV ($n = 6$; $P < 0.001$; paired t-test) were observed (Figure 1A). When DCPIB, at a concentration able to inhibit VRAC (10 µM) in cultured astrocytes (Abdullaev *et al.*, 2006), was added to the hypotonic solution a marked decrease in inward current was seen, indicating that in the negative range of membrane potentials the majority of hypotonicity-induced current was carried by VRACs (Benfenati *et al.*, 2009) (Figure 1A,B and Supporting Information Figure S1A). Surprisingly, DCPIB caused an increase in outward current and the E_0 shift to -61.4 ± 8.7 mV ($n = 6$; $P < 0.05$; paired t-test), a value closer to the equilibrium potential for K^+ under our experimental conditions ($E_K = -91$ mV). DCPIB effect was fully reversible, as upon washout with isotonic solution ramp currents quickly returned to a level similar to that before hypotonic challenge. Collectively, these results suggest that DCPIB has a dual effect on astrocytic swelling-induced current; it inhibits VRAC current and likely causes an augment in K^+ permeability.

DCPIB activates a K^+ conductance in rat primary cortical astrocytes

Because our results could not rule out that DCPIB-induced increase in membrane current was not dependent on activation of swelling-sensitive channels, we next explored the ability of DCPIB to modulate channel activity in isotonic condition. The membrane potential was clamped at V_h of –60 mV and the whole-cell currents were elicited by a ramp stimulation protocol (inset to Figure 2A) ranging from –120 to +60 mV. Under these conditions, DCPIB activated reversibly an outwardly rectifying current (Figure 2A) and induced the hyperpolarization of E_0 from -34.6 ± 1.9 to -71.3 ± 2.6 mV ($n = 9$). The onset of the effect was rapid starting within 10 s from the beginning of the DCPIB exposure, reached its maximum within 60 s ($t_{1/2}$ of activation of 35 ± 5 s; $n = 7$) and remained stable for the entire time of the

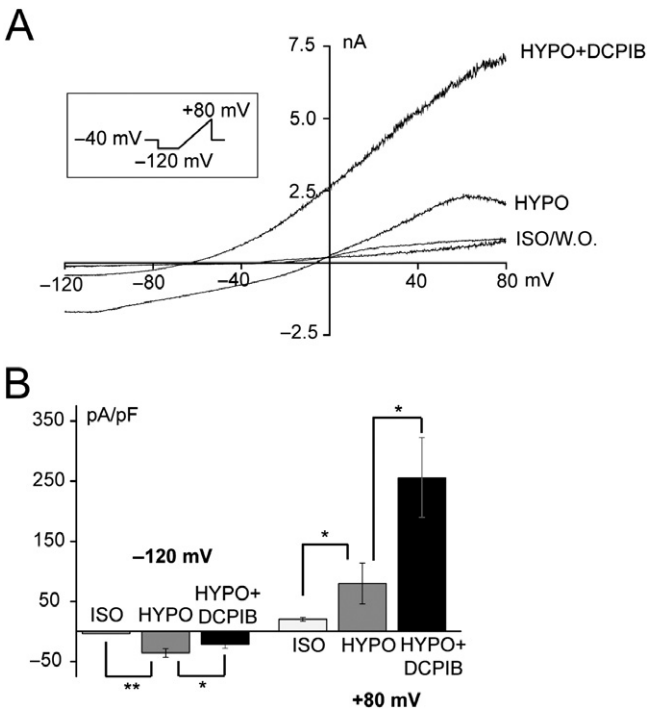

Figure 1

Effect of DCPIB on currents activated by hypotonicity in primary cultured rat cortical astrocytes. A: Representative I/V traces of whole-cell currents evoked with a voltage protocol (inset) that from a holding potential of −40 mV hyperpolarizes the membrane potential to −120 mV for 3 s before the application of a slowly depolarizing ramp to +80 mV (40 mV·s^{-1}). Addition of 10 μM DCPIB decreased the hypotonicity-induced current at −120 mV but augmented the current magnitude at +80 mV. DCPIB effect was accompanied by a large hyperpolarization of current reversal potential. Upon washout (W.O.) with isotonic solution current returned to the basal level. B: Bar graph showing current densities assessed at −120 mV and +80 mV in isotonic solution (ISO) and under hypotonic conditions (HYPO) before and after 10 μM DCPIB application ($n = 6$). Statistical significance was calculated using paired two-tailed Student's *t*-test; $^*P < 0.05$, $^{**}P < 0.01$.

application before returning to the basal level upon washout (Figure 2B). Importantly, when intra- and extracellular monovalent cations were replaced with cesium (Cs^+) DCPIB did not produce any increase of the background current (see Supporting Information Figure S1B). The DCPIB effect was dose-dependent with half-maximal activation concentration (EC_{50}) of 102 μM and Hill coefficient (n) of 2.8 (Figure 2C).

Although the data suggested that DCPIB augmented primarily the K^+ conductance, we next sought to determine the ionic selectivity by measuring the reversal potentials of ramp currents evoked under various extracellular K^+ concentrations ($[K^+]_o$). In 4 mM $[K^+]_o$ the reversal potential (E_{rev}) of the current evoked by DCPIB exposure was −76.1 ± 4.2 mV ($n = 7$). In 100 mM $[K^+]_o$ the E_{rev} of the DCPIB-induced current shifted positively to −2.3 ± 4.6 mV ($n = 6$), close to the E_{rev} change of 82 mV expected for a K^+ selective current under our experimental conditions (Figure 2D). Noteworthy, in high $[K^+]_o$ the DCPIB-induced current displayed an increase in slope conductance and adopted a linear profile suggesting that DCPIB evoked a current with biophysical properties compatible with the activation of a K^+ conductance mediated by open rectifier channels (Goldstein *et al.*, 2001).

In the attempt to identify the type of open rectifier K^+ channel activated by DCPIB, we compared the effect of DCPIB with that of AA, which previous studies demonstrated to activate the open rectifier K_{2P} 10.1 in rat primary cortical astrocytes (Gnatenco *et al.*, 2002; Ferroni *et al.*, 2003). Astrocytes were challenged with DCPIB (10 μM) and AA (10 μM). The result indicates that DCPIB activated a K^+ conductance whose kinetics resembled those of the current promoted by AA exposure (Figure 3A–C). The observation that saturating concentration of DCPIB occluded the effect of AA strongly suggests that in cultured astrocytes DCPIB and AA activated the same K^+ channel (Figure 3D). Finally, the putative blockers of TREKs quinidine and quinine (Lesage and Lazdunski, 2000) depressed both the AA- and DCPIB-induced currents (Figure 3E, F).

In order to substantiate the observation that TREK channels were involved in the positive modulation of the K^+ conductance by DCPIB we investigated the effect of zinc ion (Zn^{2+}), which previous study indicated to be an activator of recombinant K_{2P} 10.1 and K_{2P} 2.1 (Gruss *et al.*, 2004; Kim *et al.*, 2005) and to inhibit the AA-activated K_{2P} 4.1 (TRAAK) channel (Czirják and Enyedi, 2006). Micromolar concentrations of Zn^{2+} (100 μM) had a negligible effect on basal K^+ current and caused a small non-significant increase in the outward current generated by submaximal concentrations of DCPIB (Supporting Information Figure S2). These results rule out a major contribution of K_{2P} 4.1 in the activation of K_{2P} channel by DCPIB and suggest that K_{2P} 10.1 and/or K_{2P} 2.1 could be involved.

Expression of K_{2P} 2.1 and K_{2P} 10.1 channels in primary cultured rat cortical astrocytes

In order to get further insight into the molecular mechanism of DCPIB action on astroglial K^+ conductance, we next investigated the protein expression of TREK channels in cultured cortical astrocytes by immunocytochemical analysis. The data indicate the presence of K_{2P} 2.1 and K_{2P} 10.1 immunosignals in the plasma membrane as depicted by the lack of overlay signal between TREK proteins and the cytoplasmic protein GFAP (Figure 4).

DCPIB activates recombinant K_{2P} 2.1 and K_{2P} 10.1

To corroborate the hypothesis that DCPIB effect on astroglial K^+ conductance was due to K_{2P} 2.1 and K_{2P} 10.1 activation we performed a comparative functional analysis in COS-7 cells transiently transfected with recombinant rat TREK channels. COS-7 cells that were not transfected with recombinant TREK channels, but expressed the reporter gene EYFP did not respond to the application of two different DCPIB concentrations (10 μM and 30 μM) and to AA (10 μM) (data not shown). The whole-cell current density at +60 mV of EYFP-bearing COS-7 cells was 4.7 ± 1.0 pA·pF^{-1} ($n = 9$) after prolonged application of 10 μM DCPIB (Table 1). By contrast, 10 μM DCPIB rapidly induced outwardly rectifying currents that were promptly reversed upon washout in both K_{2P} 2.1/

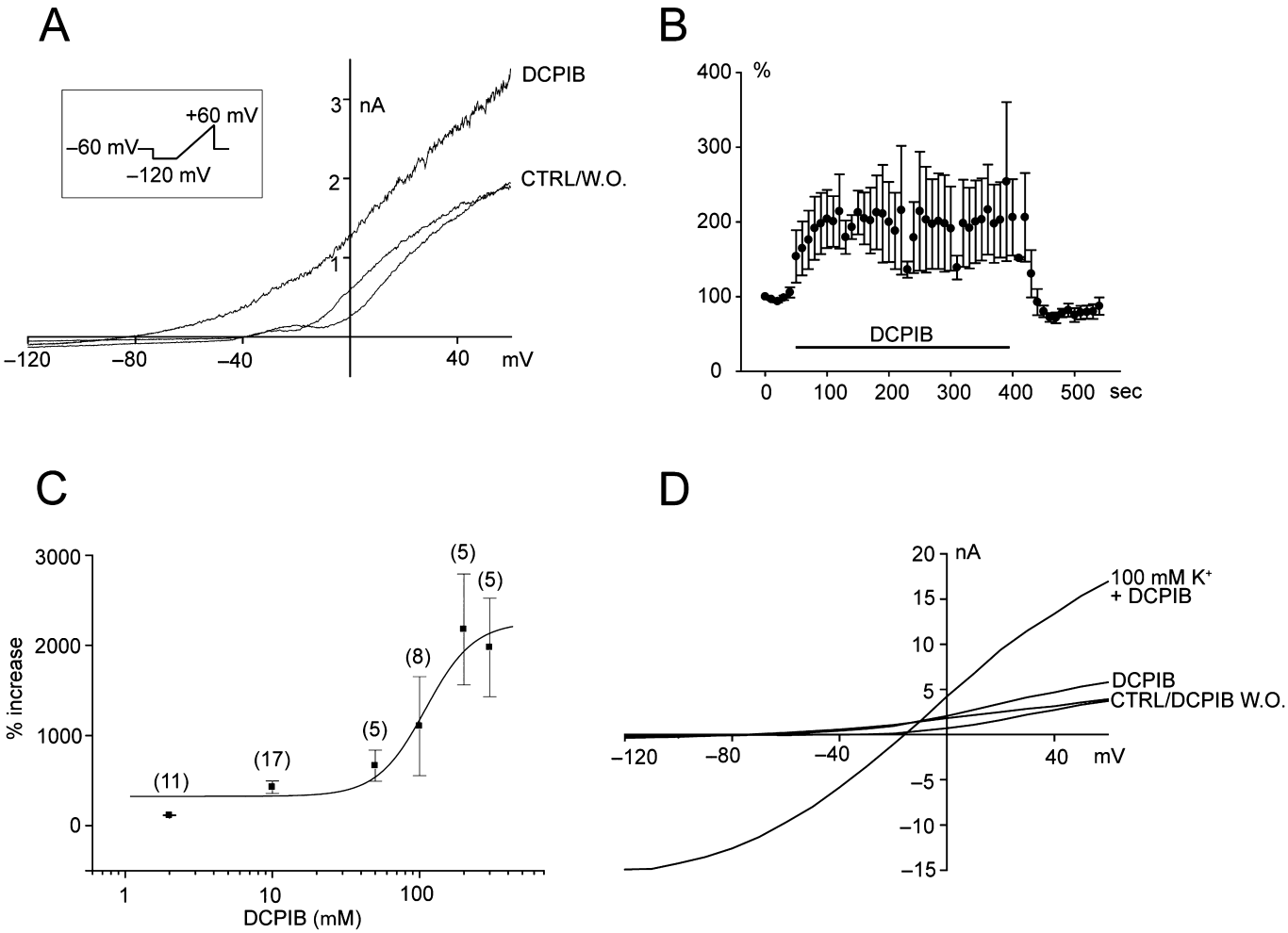

Figure 2

DCPIB activates a sustained K^+-selective current in cultured astrocytes upon isotonicity. A: Representative I/V traces of astrocyte whole-cell currents evoked with the protocol in inset in standard bath solution (CTRL), following addition of 10 μM DCPIB (DCPIB) and after washout in standard bath solution (W.O.). DCPIB increased reversibly the outward current. B: Time-course of the percentage increase in current magnitude at +60 mV upon prolonged DCPIB application compared with the current before DCPIB administration ($n = 11$). C: Dose–response curve of the current increases following DCPIB challenge. Current densities of the DCPIB-induced outward currents measured at +60 mV were normalized to the control currents in the absence of DCPIB. The percentage increase in current densities fitted to a Hill equation yields a half-maximal concentration (EC_{50}) of 102 μM and Hill coefficient of 2.8. Numbers in brackets denote sample size (n). D: Representative I/V traces of whole-cell currents measured in standard 4 mM K^+ bath solution in the absence (CTRL) and presence of 10 μM DCPIB (DCPIB) display an outwardly rectifying profile. In extracellular solution containing 100 mM K^+ the DCPIB-evoked current reversed polarity at more positive membrane potentials and became linear suggesting the activation of open rectifier K^+ channels. Currents returned outwardly rectifying after washout with the 4 mM K^+ bath solution containing DCPIB (DCPIB W.O.). The voltage protocol is the same as in A.

EYFP and K_{2P} 10.1/EYFP transfected COS-7 cells (Figure 5A, B). In K_{2P} 2.1/EYFP-transfected cells, the application of DCPIB induced an increase in whole-cell current density at +60 mV from 41.9 ± 19.1 to 122.4 ± 31.6 pA·pF^{-1} ($n = 5$; $P < 0.05$, paired t-test), and E_0 shifted from –35.2 ± 5.7 to –83.6 ± 1.8 mV after DCPIB application ($n = 5$; $P < 0.01$, paired t-test). In K_{2P} 10.1/EYFP transfected COS-7 cells, the current density increased from 13.2 ± 3.1 to 120.1 ± 47.2 pA·pF^{-1} after DCPIB application ($n = 5$; $P < 0.05$ paired t-test) and the E_0 shifted from –26.1 ± 8.9 to –71.4 ± 6.5 mV ($n = 8$; $P < 0.001$ paired t-test) (Table 1). The EC_{50} and Hill coefficient of the dose–response curves for COS-7 cells transfected with K_{2P} 2.1 and K_{2P} 10.1-expressing cells were in the range of the values yielded in astrocytes (Supporting Information Figure S3). Altogether, these results support the view that DCPIB is an activator of K_{2P} 2.1 and K_{2P} 10.1 channels and confirm that the DCPIB effect on astroglial K^+ conductance is likely due to the opening of K_{2P} 2.1 and/or K_{2P} 10.1.

To verify the specificity of DCPIB action we analysed the effect of ethacrynic acid (EA), the molecule from which DCPIB is derived (Bourke *et al.*, 1981; Cragoe *et al.*, 1982). In COS-7 cells transfected with K_{2P} 2.1 and K_{2P} 10.1 that responded to DCPIB (10 μM) application of 30 μM EA did not cause any increase in membrane conductance (Figure 5C, D). Identical results were obtained in cultured astrocytes (data not shown).

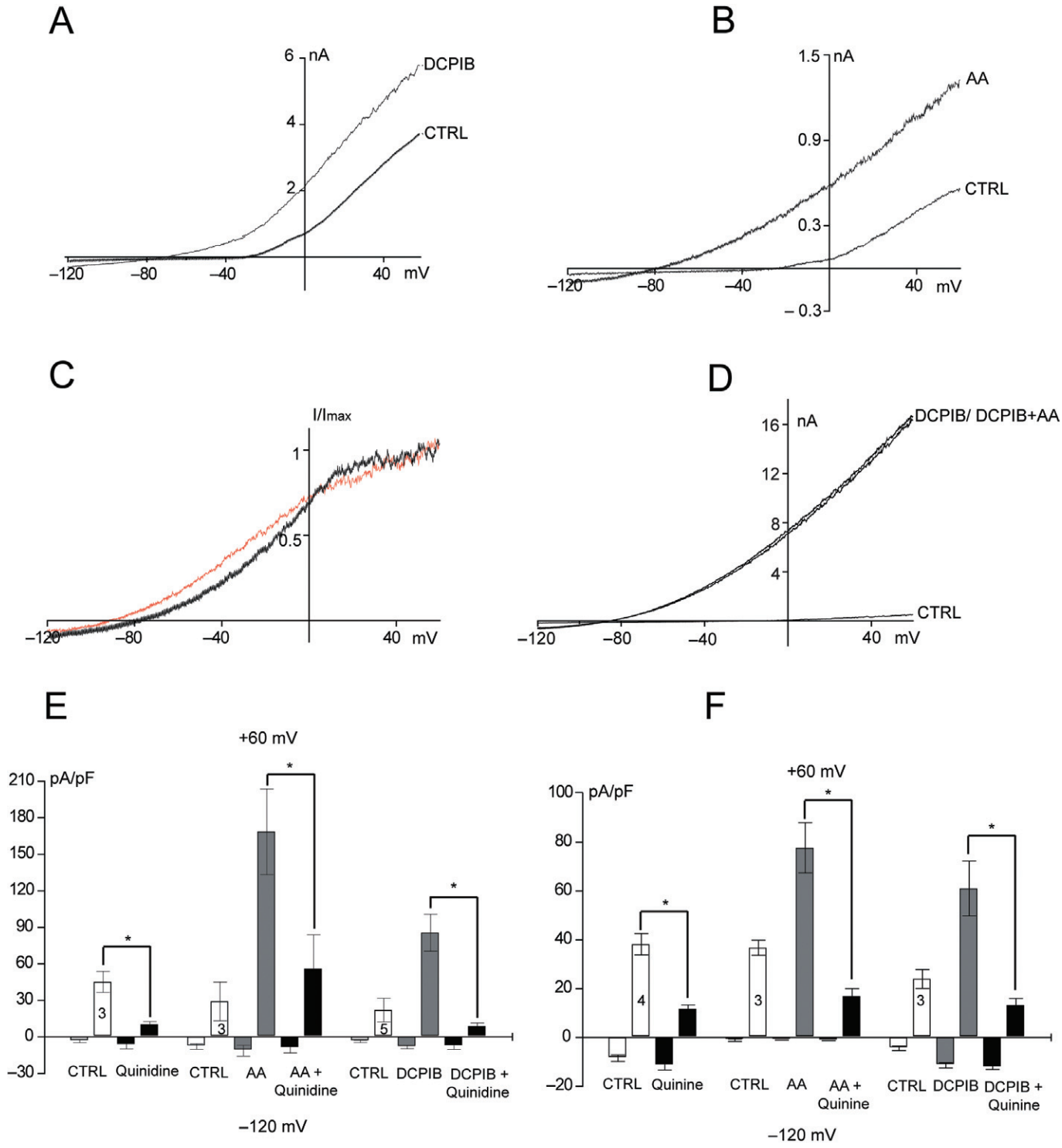

Figure 3

DCPIB stimulates TREK-mediated K^+ channels in cultured astrocytes. A–B: Representative I/V traces of control currents (CTRL) and currents evoked by DCPIB (10 μM) and AA (10 μM) in two different cells. Voltage stimulation as in Figure 2A. C: Comparison between ramp currents elicited by DCPIB (black) and AA (red). Each trace is the difference between evoked and control currents. Currents have been scaled in order to have the same amplitude at +60 mV. The result indicates that DCPIB activated a K^+ conductance whose kinetics resembled those of the AA-induced current. D: Representative I/V traces of DCPIB-evoked currents in the absence and presence of AA (10 μM). Saturating concentration of DCPIB (200 μM) caused a large increase in K^+ current which was not further augmented by co-application of AA. Voltage stimulation as in Figure 2A. E: Bar graph of K^+ current densities assessed at –120 mV and +60 mV evoked in control conditions (CTRL) and after exposure to AA or DCPIB in the absence and presence of 500 μM quinidine. F: The same as in E but following application of 200 μM quinine. Column numbers denote sample size. Statistical significance was calculated using paired two-tailed Student's *t*-test; $*P < 0.05$ compared with controls (CTRL).

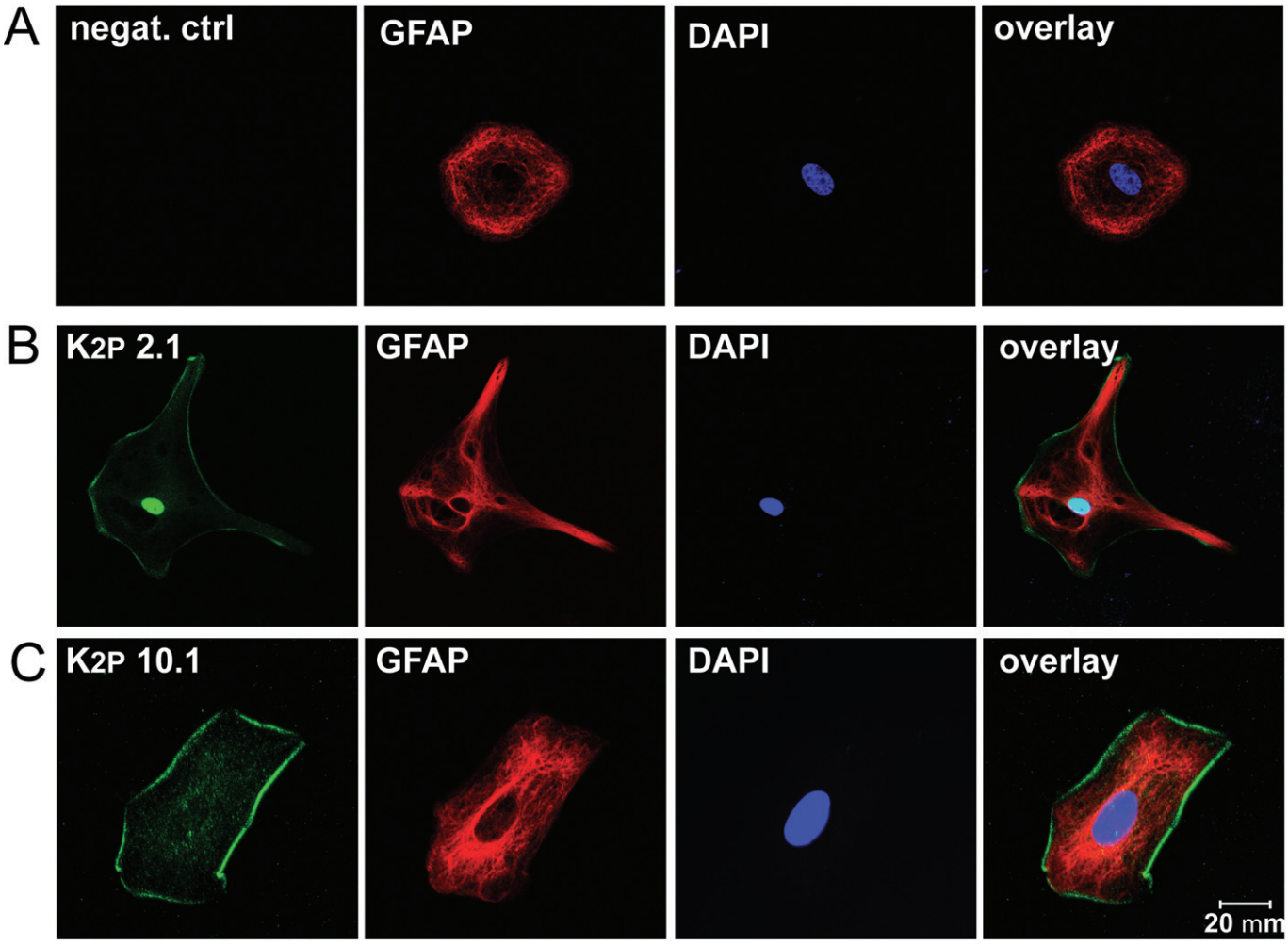

Figure 4

Cultured rat cortical astrocytes display immunosignals for K_{2P} 2.1 and K_{2P} 10.1 channel proteins A–C: Immunofluorescence staining of primary astrocyte cultures with antibodies directed against K_{2P} 2.1 (B) or K_{2P} 10.1 (C) channels and antibody against the cytosolic protein glial fibrillary acidic protein (GFAP). The two immunosignals do not overlay denoting that most of the K_{2P} 2.1 or K_{2P} 10.1 proteins are in the plasma membrane. In the absence of the primary antibodies (negat. ctrl) only GFAP was immunodetected (A). DAPI signals depict cell nuclei.

Table 1

Action of DCPIB on recombinant TREK channels

	EYFP ($n = 9$)	K_{2P} 2.1/EYFP ($n = 5$)	K_{2P} 10.1/EYFP ($n = 8$)
Before DCPIB at 60 mV (pA/pF)	4.7 ± 1.0	41.9 ± 19.1	13.2 ± 3.1
After DCPIB at 60 mV (pA/pF)	4.1 ± 1.1	122.4 ± 31.6*	120.1 ± 47.2*
E_0 before DCPIB (mV)	–15.0 ± 3.8	–35.2 ± 5.7	–26.1 ± 8.9
E_0 after DCPIB (mV)	–13.5 ± 4.2	–83.6 ± 1.8**	–71.4 ± 6.5***

Effect of DCPIB (10 μM) on membrane currents measured in COS-7 cells transfected with EYFP alone and together with K_{2P} 2.1 or K_{2P} 10.1. Values are means ± SEM of various cells (n). E_0, zero-current potential. Statistical significances are given versus COS-7 cells before DCPIB application. Paired two-tailed Student's *t*-test; *$P < 0.05$, **$P < 0.01$, ***$P < 0.001$.

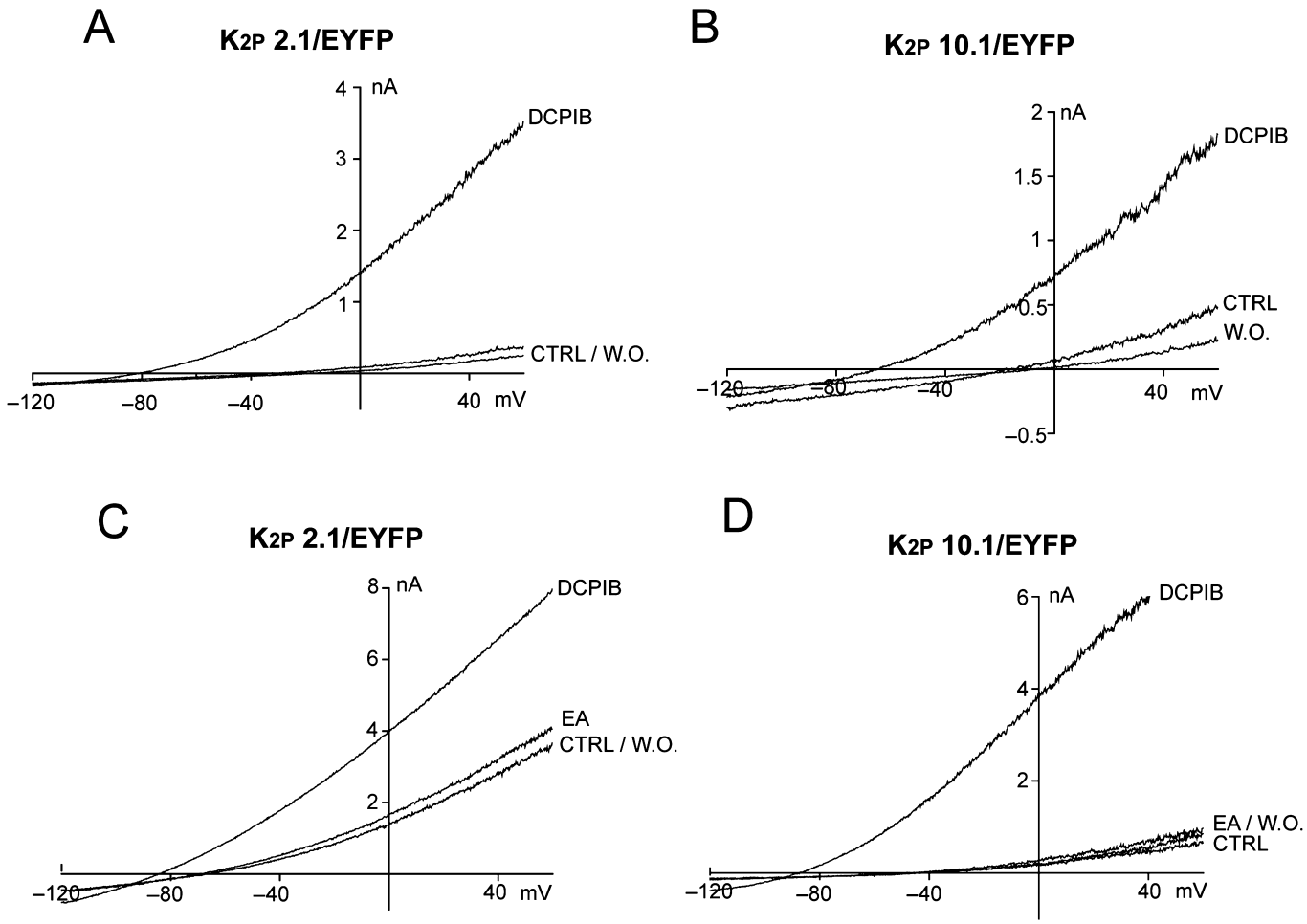

Figure 5

DCPIB but not the related molecule ethacrynic acid activates K_{2P} 2.1 and K_{2P} 10.1 channels expressed in transfected COS-7 cells. A: Representative I/V traces recorded in COS-7 cells transfected with K_{2P} 2.1 and the reporter gene EYFP (K_{2P} 2.1/EYFP) exposed to the standard bath solution (CTRL), after application of 10 μM DCPIB (DCPIB) and upon DCPIB washout with the standard bath solution (W.O.). B: Representative I/V traces of whole-cell recording in K_{2P} 10.1/EYFP-transfected cells in standard bath solution (CTRL), in the presence of 10 μM DCPIB and following washout (W.O.). C–D: Representative I/V traces of whole-cell recordings in K_{2P} 2.1/EYFP- (C) and K_{2P} 10.1/EYFP-transfected COS-7 (D) cells in standard bath solution (CTRL), after application of 30 μM EA, upon subsequent stimulation with 10 μM DCPIB, and following washout with standard bath solution (W.O.). For voltage stimulation protocol see Figure 2A.

DCPIB augments the background currents in neurons but not in astrocytes in situ

Because K_{2P} 2.1 and/or K_{2P} 10.1 channels mediate the background conductance in subpopulations of astrocytes (Seifert *et al.*, 2009; Zhou *et al.*, 2009; Pivonkova *et al.*, 2010) we sought to investigate the effect of DCPIB on membrane properties of astrocytes *in situ*. In acute brain slices from young rats (P9–P15), the immunohistochemical staining depicted expression of K_{2P} 2.1, but not of K_{2P} 10.1 in astrocytes of the stratum radiatum of the CA1 region of the hippocampus (Figure 7B, D). In these astrocytes (Figure 6A) prolonged DCPIB application (100 μM) did not promote significant changes of the very negative E_0 (−75 ± 5 mV, $n = 12$) and did not alter the large linear membrane conductance (Figure 6B). In neurons of the dentate gyrus (granular cell layer) (Figure 6C, D), which have been demonstrated to express K_{2P} 2.1 and K_{2P} 10.1 channels (Hervieu *et al.*, 2001; Talley *et al.*, 2001), application of DCPIB caused a significant hyperpolarization (in 10 out of 18 cells) from −44.8 ± 3.6 mV to −60.4 ± 3.3 mV ($P < 0.001$; paired *t*-test). Moreover, DCPIB promoted a decrease in membrane resistance from 1198 ± 115 to 550 ± 50 MOhms ($n = 10$; $P < 0.001$; paired *t*-test) and an increase in background conductance (Figure 6E). Immunohistochemical staining confirmed the expression of K_{2P} 2.1 and K_{2P} 10.1 in granule neurons of the dentate gyrus (Figure 7C, E). Collectively, these results indicate that *in situ* DCPIB generates a significant hyperpolarization and an increase in background K^+ conductance of granule neurons in dentate gyrus but it does not affect membrane properties of CA1 astrocytes.

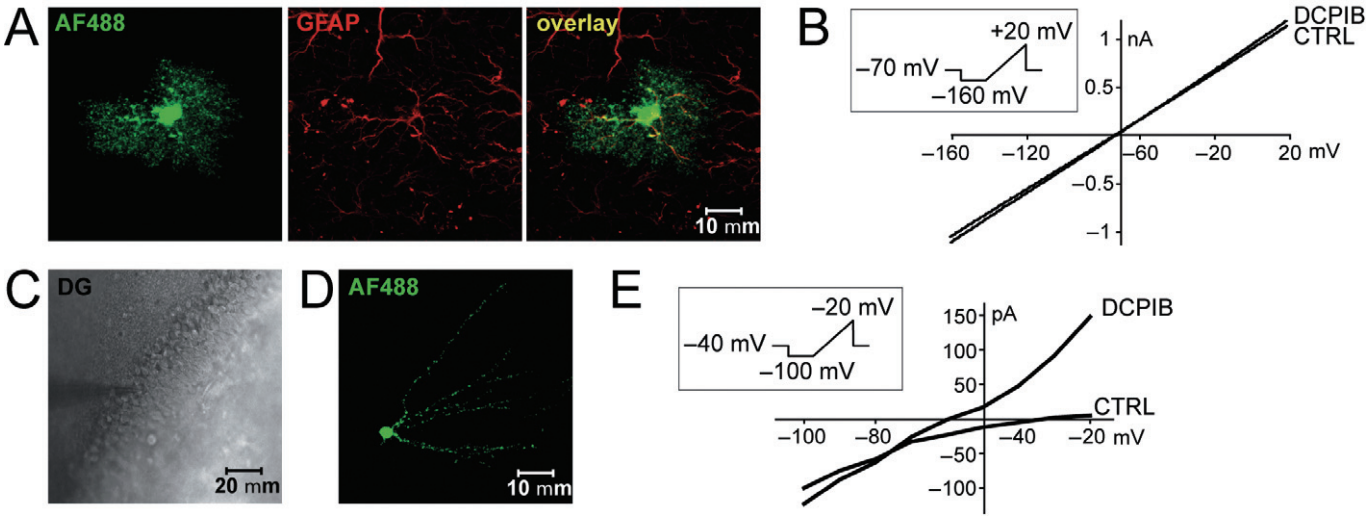

Figure 6

Effect of DCPIB application on membrane properties of astrocytes and neurons *in situ*. A: Example of an astrocyte in the CA1 region of the hippocampus (stratum radiatum) in which recordings were obtained by the whole-cell patch-clamp method, filled with Alexa Fluor 488 hydrazide (AF488) and identified using an antibody directed against glial fibrillary acidic protein (GFAP). B: I/V plots of the membrane currents evoked in a hippocampal astrocyte by a voltage ramp protocol (see inset) before (CTRL) and after application of 100 μM DCPIB. C: DCPIB-evoked currents were measured in neurons in the granular cell layer of the dentate gyrus region in young rat hippocampal slices. D: Image of a neuron measured by the whole-cell patch-clamp method and filled with Alexa Fluor 488 hydrazide (AF488) during the measurement. E: I/V plots of the currents evoked in a dentate gyrus neuron by a slow ramp depolarizing the cell membrane from –100 mV to –20 mV for 2 s (see inset), before (CTRL) and after the application of 100 μM DCPIB. Note the background current increase after DCPIB application accompanied by a substantial hyperpolarization.

Discussion

The development of astroglial swelling is a well-known reaction of the CNS to various types of injuries including trauma, ischaemia or neurointoxication (for a review see Kimelberg, 2005). Because swelling is detrimental for neuronal survival, great efforts are currently made to identify the underlying molecular mechanisms and to develop pharmacological tools able to counteract its development and/or to promote the process of volume recovery called regulatory volume decrease (RVD). VRACs have been identified as crucial players in the complex series of events leading to cell volume recovery in many cell types (Eggermont *et al.*, 2001). In astroglial cells VRAC inhibition was reported to depress the excitotoxic release of glutamate and aspartate (Abdullaev *et al.*, 2006). In support of the central role of VRAC in brain excitotoxicity, there is substantial evidence that the neuroprotective molecule DCPIB inhibits VRAC channels in cultured astrocytes (Abdullaev *et al.*, 2006). Our work shows that in primary cultured astrocytes, DCPIB not only affects the hypotonicity-induced Cl^- conductance, but also stimulates K^+ channels belonging to the TREK subfamily of the large K_{2P} family, which might be involved in the homeostatic control of astroglial cells. We also report that DCPIB positively modulates the background K^+ conductance of neurons *in situ*. These results identify novel molecular targets of DCPIB, which might be relevant for the neuroprotective role of DCPIB *in vivo*.

Previous research addressing the effect of DCPIB on K^+ conductance reported that DCPIB did not modulate K^+ channels in guinea pig atrial cardiomyocytes (Decher *et al.*, 2001). In rat pancreatic β-cells, DCPIB inhibited VRACs and activated ATP-dependent K^+ channels (K_{ATP}) via an indirect mechanism (Best *et al.*, 2004). Although the DCPIB effect on astroglial K^+ conductance was observed under conditions of isotonicity, from our study we cannot rule out that it is the consequence of its interaction with VRACs. In extracellular isotonic solution VRAC currents were negligible and upon hypotonicity they were fully depressed by DCPIB concentrations that activated the K^+ conductance.

The conclusion that DCPIB stimulates K_{2P} channels of the TREK subfamily is supported by two lines of evidence: (i) the negative shift in reversal potential of the DCPIB-induced current towards the Nernst equilibrium potential for K^+ and the change in rectification properties under high extracellular K^+ typical of open rectifier K_{2P} channels; and (ii) the result that saturating concentrations of DCPIB occluded the activation of the K^+ conductance by AA that previous studies in cultured astrocytes showed to be mediated by K_{2P} 10.1 channel (Gnatenco *et al.*, 2002; Ferroni *et al.*, 2003). Furthermore, quinidine and quinine, two known blockers of TREK channels (Lesage and Lazdunski, 2000), also strongly depressed the AA- and DCPIB-evoked currents.

It was previously reported that cultured astrocytes express the mRNA of K_{2P} 10.1, but not of K_{2P} 2.1 (Gnatenco *et al.*, 2002; Ferroni *et al.*, 2003). Here we depicted immunosignal for both K_{2P} 10.1 and K_{2P} 2.1 in cultured astroglia. This discrepancy could be explained by the former use of primers unable to detect the K_{2P} 2.1 isoforms present in these cells. Our results are consistent with recent studies showing the expression of K_{2P} 10.1 and K_{2P} 2.1 in primary cultured

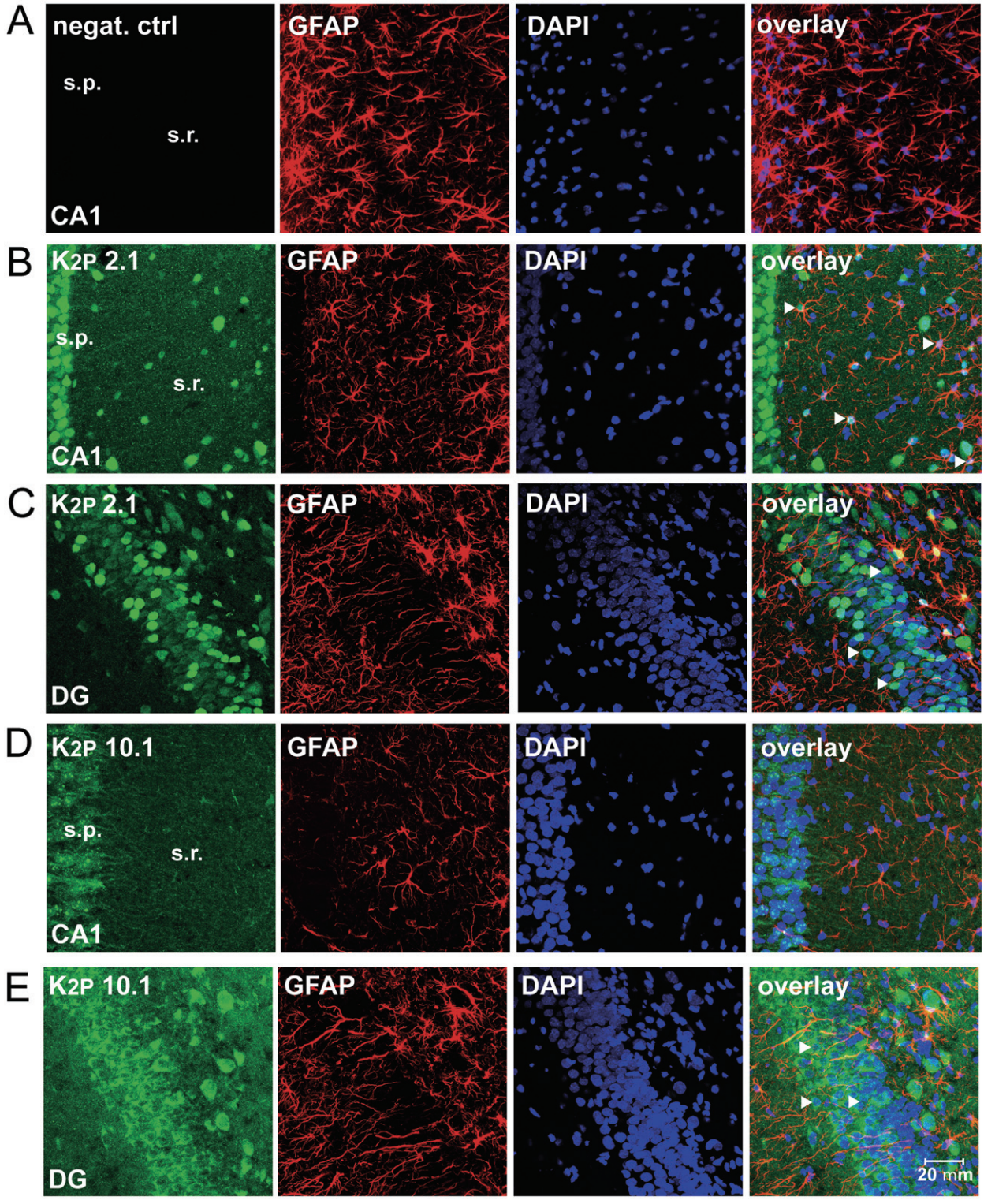

Figure 7

Immunolocalization of K_{2P} 2.1 and K_{2P} 10.1 proteins in hippocampal slices. A: Representative negative control (negat. ctrl) of immunostaining in the absence of primary antibodies against channel proteins. B: Immunohistochemical staining of fixed brain sections against K_{2P} 2.1 and glial fibrillary acidic protein (GFAP) in the CA1 region of the hippocampus. Arrowheads indicate positively-stained astrocytes. (s.p. – stratum pyramidale; s.r. – stratum radiatum) C: Staining for K_{2P} 2.1 and GFAP in the dentate gyrus. Arrowheads indicate positively-stained neurons. D: Immunohistochemical staining of fixed brain sections against K_{2P} 10.1 and GFAP in the CA1 region of the hippocampus. (s.p. – stratum pyramidale; s.r. – stratum radiatum) E: Staining for K_{2P} 10.1 channels and GFAP in the dentate gyrus. Arrowheads indicate positively stained neurons. DAPI signals in A–E depict cell nuclei.

astrocytes (Kucheryavykh *et al.*, 2009; Wang *et al.*, 2012) and *in situ* (Seifert *et al.*, 2009). The identity of K^+ channels activated by DCPIB was also addressed by complementary expression experiments of recombinant K_{2P} 2.1 and K_{2P} 10.1 in COS-7 cells. The comparison of the DCPIB-evoked current kinetics and DCPIB sensitivity in cultured rat cortical astrocytes and in TREK-transfected cells suggest that the DCPIB effect on K^+ conductance in astrocytes is most likely mediated by K_{2P} 2.1 and K_{2P} 10.1 channels. This view is further supported by the result that administration of Zn^{2+}, which stimulates the activity of recombinant K_{2P} 2.1 and K_{2P} 10.1 (Gruss *et al.*, 2004; Kim *et al.*, 2005), promoted a small but non-significant increase of DCPIB current in cultured astrocytes. This observation also rules out the possibility that K_{2P} 4.1, another member of the K_{2P} channel family also activated by AA, contributes substantially to the DCPIB-induced K^+ current increase because K_{2P} 4.1 is inhibited by Zn^{2+} (Czirják and Enyedi, 2006). Moreover, K_{2P} 4.1 was reported to be absent in astroglia *in situ* (Seifert *et al.*, 2009) and recombinant K_{2P} 4.1 showed no significant activation by 10 μM DCPIB (our unpublished observation).

DCPIB is considered an hydrophobic drug (Best *et al.*, 2004) and therefore it also could affect TREK channels acting on the intracellular leaflet of the plasma membrane. However, the rapid onset of current activation and deactivation upon DCPIB challenge, the multiple activation upon repetitive applications and the failure of intracellular DCPIB to evoke any significant effect on background conductance of cortical rat astrocytes (our unpublished results) render this hypothesis unlikely. The finding that ethacrynic acid, from which DCPIB is derived, did not activate either recombinant K_{2P} 2.1 and K_{2P} 10.1 transfected in COS-7 cells or any K^+ current in rat cortical astrocytes, demonstrates that the effect of DCPIB is mediated by a functional group that is not present in ethacrynic acid. Further studies are necessary to identify other molecules with a backbone structure similar to ethacrynic acid which could mimic the DCPIB action on TREK channels.

The K_{2P} channels are highly expressed in the nervous system (Medhurst *et al.*, 2001). In the rodent brain, TREK channels are present in the cerebellum and hippocampus (Talley *et al.*, 2001; Aller and Wisden, 2008). Although they are predominantly found in some subpopulations of neurons, TREK channels were recently detected also in astrocytes *in situ* (Seifert *et al.*, 2009; Zhou *et al.*, 2009; Pivonkova *et al.*, 2010). In the astrocytic population of the grey and white matter, TREK together with TWIK1 and Kir4.1 channels, contribute to the large background K^+ conductance and to the setting of the highly negative resting membrane potential. These parameters are critical for the process of extracellular K^+ clearance necessary for maintaining the extracellular K^+ homeostasis and for tuning neuronal activity under physiological conditions and during ischemia when extracellular K^+ concentration increases up to 80 mM (Somjen, 1979). It has been reported that downregulation of Kir4.1 channels by RNA interference promoted a reduction in K^+ buffer capacity in cortical astrocytes (Kucheryavykh *et al.*, 2007). In Muller glial cells of retina the expression of Kir4.1 protein and the relevant whole-cell K^+ currents are strongly downregulated after transient ischemia (Iandiev *et al.*, 2006). By contrast, K_{2P} 2.1 and K_{2P} 10.1 mRNA as well as protein expression increase in both hippocampus and cortex 24 h after MCAO (Li *et al.*, 2005; Wang *et al.*, 2012). Finally, K_{2P} 10.1 is up-regulated in cortical astrocytes after *in vitro* experimental ischemia (Kucheryavykh *et al.*, 2009). Taken together, these data suggest that following hypoxia/ischemia, Kir4.1 and TREK channels are reciprocally regulated. It can be envisaged that activation of TREK channels in astrocytes is likely to play a major role following primary ischemia when TREK could be the dominant K^+ conductance around the resting membrane potential.

Cultured astrocytes lack functional Kir channels (Gray and Ritchie, 1986; Ferroni *et al.*, 1995) and display several properties of reactive astroglia (McMillian *et al.*, 1994; Wu and Schwartz, 1998). Because DCPIB caused a strong decrease in input resistance and a large hyperpolarization of astrocyte membrane potential, in reactive astroglia the DCPIB-induced increase in TREK activity would provide an efficient mechanism to buffer high extracellular K^+ and to set the negative membrane potential which favours glutamate uptake (Kucheryavykh *et al.*, 2009). Whether the increase in TREK-mediated K^+ conductance by DCPIB augments the efficacy of RVD following astrocyte swelling remains to be established. Future studies shall also address the role of DCPIB-induced increase of astroglial K^+ conductance in cell proliferation. There is evidence, in fact, that in cultured astrocytes an increase in K^+ conductance produces the arrest of proliferative process (Higashimori and Sontheimer, 2007). Moreover, a recent study showed that in cultured astrocytes DCPIB depressed astroglial proliferation and modulated cell cycle progression, even though such effects were attributed to DCPIB-induced blockage of VRACs (He *et al.*, 2012).

In our *in situ* study, the negative resting membrane potential close to the E_K and the low input resistance denote the presence of a high background K^+ conductance in hippocampal astrocytes. There is substantial evidence that operative TREK channels contribute to this background conductance (Seifert *et al.*, 2009; Zhou *et al.*, 2009), and thus it was not surprising to observe that DCPIB did not have any detectable effect in astroglia *in situ*. Further studies will address whether astroglia of other brain regions are able to respond to DCPIB challenge. Since in slices the resting membrane potential of neurons is relatively far from E_K, it is conceivable that neuronal TREK channels *in situ* are largely not operative. The observation that DCPIB increased the background conductance and hyperpolarized neuronal resting membrane potential substantiates the view that DCPIB is also able to depress neuronal excitability. Collectively, the results underscore the possibility that the neuroprotective effect of DCPIB observed after MCAO (Zhang *et al.*, 2008) is due, at least in part, to the activation of TREK channels in neurons and astroglial cells.

Conclusions

Our work demonstrates that the neuroprotective molecule DCPIB causes the activation of certain K_{2P} channels in cultured astrocytes and neurons *in situ*. These results are important because the relationship between variations in K_{2P} channel activity and the pathogenesis of several diseases is becoming clear (Es-Salah-Lamoureux *et al.*, 2010), and the search for K_{2P} channels activators and inhibitors as therapeutic agents has become a high priority (Mathie and Veale,

2007). This study identifies DCPIB as a novel activator of TREK channels that could be used as template to synthesize novel pharmacological tools able to specifically increase the activity of some K_{2P} channel subtypes. In the context of neurological diseases that can be treated by modulating TREK channel activity the potential therapeutic value of DCPIB and other related compounds is worth to be explored and deserves further investigation.

Acknowledgements

This work was supported by grants from MIUR (Italy) to S.F., Progetti Strategici di Ateneo 2007 (University of Bologna) to M.C., and by grant from the Grant Agency of the Czech Republic (CZ : GA CR : GAP303/10/1338) to M.A. We thank Alessia Minardi for preparation and maintenance of primary cultures of cortical astrocytes and Anna Utili and Pavel Honsa for technical assistance.

Conflict of interest

None.

References

Abdullaev IF, Rudkouskaya A, Schools GP, Kimelberg HK, Mongin AA (2006). Pharmacological comparison of swelling-activated excitatory amino acid release and Cl- currents in cultured rat astrocytes. J Physiol 572: 677–689.

Aller MI, Wisden W (2008). Changes in expression of some two-pore domain potassium channel genes (KCNK) in selected brain regions of developing mice. Neuroscience 151: 1154–1172.

Benesova J, Hock M, Butenko O, Prajerova I, Anderova M, Chvatal A (2009). Quantification of astrocyte volume changes during ischemia in situ reveals two populations of astrocytes in the cortex of GFAP/EGFP mice. J Neurosci Res 87: 96–111.

Benesova J, Rusnakova V, Honsa P, Pivonkova H, Dzamba D, Kubista M *et al.* (2012). Distinct expression/function of potassium and chloride channels contributes to the diverse volume regulation in cortical astrocytes of GFAP/EGFP mice. Plos ONE 7: e29725.

Benfenati V, Caprini M, Nicchia GP, Rossi A, Dovizio M, Cervetto C *et al.* (2009). Carbenoxolone inhibits volume-regulated anion conductance in cultured rat cortical astroglia. Channels 3: 323–336.

Best L, Yates AP, Decher N, Steinmeyer K, Nilius B (2004). Inhibition of glucose-induced electrical activity in rat pancreatic beta-cells by DCPIB, a selective inhibitor of volume-sensitive anion currents. Eur J Pharmacol 489: 13–19.

Bourke RS, Waldman JB, Kimelberg HK, Barron KD, San Filippo BD, Popp AJ *et al.* (1981). Adenosine-stimulated astroglial swelling in cat cerebral cortex in vivo with total inhibition by a non-diuretic acylaryloxyacid derivative. J Neurosurg 55: 364–370.

Caprini M, Ferroni S, Planells-Cases R, Rueda J, Rapisarda C, Ferrer-Montiel A *et al.* (2001). Structural compatibility between the putative voltage sensor of voltage-gated K^+ channels and the prokaryotic KcsA channel. J Biol Chem 276: 21070–21076.

Cragoe EJ Jr, Gould NP, Woltersdorf OW Jr, Ziegler C, Bourke RS, Nelson LR *et al.* (1982). Agents for the treatment of brain injury. 1. (Aryloxy)alkanoic acids. J Med Chem 25: 567–579.

Czirják G, Enyedi P (2006). Zinc and mercuric ions distinguish TRESK from the other two-pore-domain K^+ channels. Mol Pharmacol 69: 1024–1032.

Decher N, Lang HJ, Nilius B, Bruggemann A, Busch AE, Steinmeyer K (2001). DCPIB is a novel selective blocker of I(Cl,swell) and prevents swelling-induced shortening of guinea-pig atrial action potential duration. Br J Pharmacol 134: 1467–1479.

Duprat F, Lesage F, Patel AJ, Fink M, Romey G, Lazdunski M (2000). The neuroprotective agent riluzole activates the two P domain K^+ channels TREK-1 and TRAAK. Mol Pharmacol 57: 906–912.

Eggermont J, Trouet D, Carton I, Nilius B (2001). Cellular function and control of volume-regulated anion channels. Cell Biochem Biophys 35: 263–274.

Es-Salah-Lamoureux Z, Steele DF, Fedida D (2010). Research into the therapeutic roles of two-pore-domain potassium channels. Trends Pharmacol Sci 31: 587–595.

Ferroni S, Marchini C, Schubert P, Rapisarda C (1995). Two distinct inwardly rectifying conductances are expressed in long term dibutyryl-cyclic-AMP treated rat cultured cortical astrocytes. FEBS Lett 367: 319–325.

Ferroni S, Valente P, Caprini M, Nobile M, Schubert P, Rapisarda C (2003). Arachidonic acid activates an open rectifier potassium channel in cultured rat cortical astrocytes. J Neurosci Res 72: 363–372.

Feustel PJ, Jin Y, Kimelberg HK (2004). Volume-regulated anion channels are the predominant contributors to release of excitatory amino acids in the ischemic cortical penumbra. Stroke 35: 1164–1168.

Gnatenco C, Han J, Snyder AK, Kim D (2002). Functional expression of TREK-2 K^+ channel in cultured rat brain astrocytes. Brain Res 931: 56–67.

Goldstein SA, Bockenhauer D, O'Kelly I, Zilberberg N (2001). Potassium leak channels and the KCNK family of two-P-domain subunits. Nat Rev Neurosci 2: 175–184.

Gray PT, Ritchie JM (1986). A voltage-gated chloride conductance in rat cultured astrocytes. Proc R Soc Lond B Biol Sci 228: 267–288.

Gruss M, Mathie A, Lieb WR, Franks NP (2004). The two-pore-domain K^+ channels TREK-1 and TASK-3 are differentially modulated by copper and zinc. Mol Pharmacol 66: 530–537.

Hamill OP, Marty A, Neher E, Sakmann B, Sigworth FJ (1981). Improved patch-clamp techniques for high-resolution current recording from cells and cell-free membrane patches. Pflugers Arch 391: 85–100.

He D, Luo X, Wei W, Xie M, Wang W, Yu Z (2012). DCPIB, a specific inhibitor of volume-regulated anion channels (VRACs), inhibits astrocyte proliferation and cell cycle progression via G1/S arrest. J Mol Neurosci 46: 249–257.

Hervieu GJ, Cluderay JE, Gray CW, Green PJ, Ranson JL, Randall AD *et al.* (2001). Distribution and expression of TREK-1, a two-pore-domain potassium channel, in the adult rat CNS. Neuroscience 103: 899–919.

Higashimori H, Sontheimer H (2007). Role of Kir4.1 channels in growth control of glia. Glia 55: 1668–1679.

Iandiev I, Tenckhoff S, Pannicke T, Biederman B, Hollborn M, Wiedemann P *et al.* (2006). Differential regulation of Kir4.1 and Kir2.1 expression in the ischemic rat retina. Neurosci Lett 396: 97–101.

Judge SI, Smith PJ (2009). Patents related to therapeutic activation of K(ATP) and K(2P) potassium channels for neuroprotection: ischemic/hypoxic/anoxic injury and general anesthetics. Expert Opin Ther Pat 19: 433–460.

Kahle KT, Simard JM, Staley KJ, Nahed BV, Jones PS, Sun D (2009). Molecular mechanisms of ischemic cerebral edema: role of electroneutral ion transport. Physiology (Bethesda) 24: 257–265.

Kim JS, Park JY, Kang HW, Lee EJ, Bang H, Lee JH (2005). Zinc activates TREK-2 potassium channel activity. J Pharmacol Exp Ther 314: 618–625.

Kimelberg HK (2005). Astrocytic swelling in cerebral ischemia as a possible cause of injury and target for therapy. Glia 50: 389–397.

Kimelberg HK, Nestor NB, Feustel PJ (2004). Inhibition of release of taurine and excitatory amino acids in ischemia and neuroprotection. Neurochem Res 29: 267–274.

Kucheryavykh LY, Kucheryavykh YV, Inyushin M, Shuba YM, Sanabria P, Cubano LA *et al.* (2009). Ischemia increases TREK-2 channel expression in astrocytes: relevance to glutamate clearance. Open Neurosci J 3: 40–47.

Kucheryavykh YV, Kucheryavykh LY, Nichols CG, Maldonado HM, Baksi K, Reichenbach A *et al.* (2007). Downregulation of Kir4.1 inward rectifying potassium channel subunits by RNAi impairs potassium transfer and glutamate uptake by cultured cortical astrocytes. Glia 55: 274–281.

Lawson K, McKay NG (2006). Modulation of potassium channels as a therapeutic approach. Curr Pharm Des 12: 459–470.

Lesage F, Lazdunski M (2000). Molecular and functional properties of two-pore-domain potassium channels. Am J Physiol Renal Physiol 279: F793–F801.

Li ZB, Zhang HX, Li LL, Wang XL (2005). Enhanced expressions of arachidonic acid-sensitive tandem-pore domain potassium channels in rat experimental acute cerebral ischemia. Biochem Biophys Res Commun 327: 1163–1169.

Lipton P (1999). Ischemic cell death in brain neurons. Physiol Rev 79: 1431–1568.

McMillian MK, Thai L, Hong JS, O'Callaghan JP, Pennypacker KR (1994). Brain injury in a dish: a model for reactive gliosis. Trends Neurosci 7: 138–142.

Mathie A, Veale EL (2007). Therapeutic potential of neuronal two-pore domain potassium-channel modulators. Curr Opin Investig Drugs 8: 555–562.

Medhurst AD, Rennie G, Chapman CG, Meadows H, Duckworth MD, Kelsell RE *et al.* (2001). Distribution analysis of human two pore domain potassium channels in tissues of the central nervous system and periphery. Brain Res Mol Brain Res 86: 101–114.

Minieri L, Pivonkova H, Caprini M, Anderova M, Ferroni S (2011). The inhibitor of volume-regulated anion channels DCPIB activates TREK potassium channels in cultured astrocytes. Glia 89 (Suppl. 1): P4–08.

Nilius B, Droogmans G (2003). Amazing chloride channels: an overview. Acta Physiol Scand 177: 119–147.

Parkerson KA, Sontheimer H (2003). Contribution of chloride channels to volume regulation of cortical astrocytes. Am J Physiol Cell Physiol 284: 1460–1467.

Parkerson KA, Sontheimer H (2004). Biophysical and pharmacological characterization of hypotonically activated chloride currents in cortical astrocytes. Glia 46: 419–436.

Pasantes-Morales H, Murray RA, Lilja L, Morán J (1994). Regulatory volume decrease in cultured astrocytes. I. Potassium- and chloride-activated permeability. Am J Physiol 266: C165–C171.

Pasantes-Morales H, Lezama RA, Ramos-Mandujano G, Tuz KL (2006). Mechanisms of cell volume regulation in hypo-osmolality. Am J Med 119: S4–S11.

Patel AJ, Honore E (2001). Properties and modulation of mammalian 2P domain K^+ channels. Trends Neurosci 24: 339–346.

Phillis JW, O'Regan MH (2003). Characterization of modes of release of amino acids in the ischemic/reperfused rat cerebral cortex. Neurochem Int 43: 461–467.

Pivonkova H, Benesova J, Butenko O, Chvatal A, Anderova M (2010). Impact of global cerebral ischemia on K^+ channel expression and membrane properties of glial cells in the rat hippocampus. Neurochem Int 57: 783–794.

Seifert G, Huttmann K, Binder DK, Hartmann C, Wyczynski A, Neusch C *et al.* (2009). Analysis of astroglial K^+ channel expression in the developing hippocampus reveals a predominant role of the Kir4.1 subunit. J Neurosci 29: 7474–7488.

Somjen GG (1979). Extracellular potassium in the mammalian central nervous system. Annu Rev Physiol 41: 159–177.

Talley EM, Solorzano G, Lei Q, Kim D, Bayliss DA (2001). CNS distribution of members of the two-pore-domain (KCNK) potassium channel family. J Neurosci 21: 7491–7505.

Vazquez-Juarez E, Hernandez-Benitez R, Lopez-Dominguez A, Pasantes-Morales H (2009). Thrombin potentiates D-aspartate efflux from cultured astrocytes under conditions of K^+ homeostasis disruption. J Neurochem 111: 1398–1408.

Wang M, Song J, Xiao W, Yang L, Yuan J, Wang W *et al.* (2012). Changes in lipid-sensitive two-pore domain potassium channel TREK-1 expression and its involvement in astrogliosis following cerebral ischemia in rats. J Mol Neurosci 46: 384–392.

Wu VW, Schwartz JP (1998). Cell culture models for reactive gliosis: new perspectives. J Neurosci Res 51: 675–681.

Zhang Y, Zhang H, Feustel PJ, Kimelberg HK (2008). DCPIB, a specific inhibitor of volume regulated anion channels (VRACs), reduces infarct size in MCAo and the release of glutamate in the ischemic cortical penumbra. Exp Neurol 210: 514–520.

Zhou M, Xu G, Xie M, Zhang X, Schools GP, Ma L *et al.* (2009). TWIK-1 and TREK-1 are potassium channels contributing significantly to astrocyte passive conductance in rat hippocampal slices. J Neurosci 29: 8551–8564.

Supporting information

Additional Supporting Information may be found in the online version of this article at the publisher's web-site:

Figure S1 Effect of DCPIB on astroglial Cl^- conductance. A: Representative traces of whole-cell currents in cultured cortical astrocytes evoked with a protocol (inset) that from a holding potential of 0 mV steps the membrane potential to –120 mV for 3 s before the application of a slowly depolarizing ramp to +80 mV. To isolate the Cl^- conductance symmetrical intra- and extracellular Cl^- saline solutions in which cations Na^+ and K^+ were replaced by cesium (Cs^+) were used. Under isotonic conditions (ISO CsCl) current was small and hypotonic challenge (HYPO CsCl) caused a current increase

in the whole range of membrane potentials. Addition of DCPIB (10 μM) to the hypotonic solution (HYPO CsCl + DCPIB) induced a marked decrease in both inward and outward currents. B: Representative traces of basal Cl^- current measured in isotonic solution in the absence (ISO CsCl) and presence of DCPIB (ISO CsCl + DCPIB). The DCPIB application for 5 min upon isotonicity did not cause any significant augment in membrane conductance.

Figure S2 Effect of zinc on DCPIB-activated ramp current. A 5 min application of zinc (Zn^{2+}; 100 μM) alone and together with DCPIB did not produce significant changes in basal and DCPIB-evoked currents at +60 and −120 mV.

Figure S3 Dose-response curves of the DCPIB-induced currents in transfected COS-7 cells. A: Current densities of the DCPIB-induced outward currents at +60 mV were normalized to control currents in the absence of DCPIB in K_{2P} 2.1-transfected cells. The percent increases in current density were plotted against the DCPIB concentration and fitted to a Hill equation yielding the half-maximal concentration (EC_{50}) of 27.4 μM and Hill coefficient of 1.3. Numbers in brackets denote sample size (n). B: The same as in A but in K_{2P} 10.1-transfected cells depicting the EC_{50} of 42.8 μM and Hill coefficient of 2.9.